RA'EGA
O ESPAÇO GEOGRÁFICO EM ANÁLISE
https://revistas.ufpr.br/raega

ISSN eletrônico 2177-2738
RA'EGA, Curitiba, PR, V.61, n.1, p. 29 – 47, 12/2024
http://dx.doi.org/10.5380/raega.v61i1.96603

Hydraulic dynamics of the Regolithic Neosol in the Cerrado of the Serra da Canastra National Park-MG

Dinâmica hídrica de Neossolo Regolítico em ambiente de Cerrado do Parque Nacional da Serra da Canastra-MG

Jefferson Gomes Confessor [*], Lara Luiza Silva[**], Silvio Carlos Rodrigues[***]

[*]Institute of Geography, Federal University of Catalão, jgconfessor01@gmail.com
[**]Institute of Geography, Federal University of Uberlândia, laraluiza97@hotmail.com
[***]Institute of Geography, Federal University of Uberlândia, silgel@ufu.br

http://dx.doi.org/10.5380/raega.v61i1.96603

Abstract

The knowledge of soil water dynamics, as elements are added, removed, and transformed, is an aid to understanding the processes at play in landscapes. Understanding the functioning of natural environments not only contributes to comprehending the natural dynamics of systems but also serves as a reference for adopting measures in areas at different stages of degradation. In this sense, this study sought to analyze the physical/hydraulic characteristics of the Regolithic Neosol in the Serra da Canastra National Park, MG. For this purpose, two different models of field infiltrators were used: namely a rain simulator and a concentric ring infiltrometer. Results involving the use of a rain simulator indicated high soil infiltration capacity (99.31%) even when subjected to high-intensity events (57.4 mm/h). The ring infiltrometer revealed high values of basic infiltration velocity (317.58 mm/h). These values indicate that despite being shallow (20 cm), the soil, characterized by coarse material (sand and lateritic gravel), has a high capacity to incorporate water precipitated into the profile, generating subsurface lateral flows between the higher and lower parts of the slope and causing the movement of iron along with underground water flow.

Keywords:
Infiltration, Soil water, Infiltrometer, Rainfall simulator.

Resumo

O conhecimento da dinâmica hídrica dos solos auxilia na compreensão dos processos atuantes nas paisagens, visto que a água em seu movimento adiciona, remove e transforma elementos. O entendimento do funcionamento de ambientes naturais além de corroborar na compreensão da dinâmica natural dos sistemas também se torna referencial para adoção de medidas em áreas sob diferentes estágios de degradação. Neste sentido, este estudo teve por objetivo de analisar as características físico/hídricas de um Neossolo Regolítico inserido em ambiente de Cerrado do Parque Nacional da Serra da Canastra-MG. Para tal foram utilizados dois modelos distintos de infiltrômetros de campo, sendo um simulador de chuvas e um infiltrômetro de anéis concêntricos. Os resultados

ISSN eletrônico 2177-2738
RA'EGA, Curitiba, PR, V.61, n.1, p. 29 – 47, 12/2024
http://dx.doi.org/10.5380/raega.v61i1.96603

envolvendo o uso do simulador de chuvas indicou alta capacidade de infiltração do solo (99,31%) mesmo quando submetido a eventos de alta intensidade (57,4 mm/h). O infiltrômetro de anéis revelou elevados volumes de velocidade básica de infiltração (317,58 mm/h). Os valores indicam que apesar de pouco espesso (20 cm), o solo caracterizado por material grosseiro (areais e cascalhos lateríticos) possui alta capacidade de incorporar a água precipitada no perfil, gerando fluxos laterais em subsuperfície entre as partes mais altas e baixas da vertente, realizando a movimentação do elemento Fe junto ao fluxo de água subterrâneo.

Palavras-chave:
Infiltração, Água do solo, Simulador de chuvas.

I. INTRODUCTION

Water is a crucial element that significantly influences the processes of landscape formation and transformation (LE MAITRE et al., 2007). Through its movement, water facilitates the addition, alteration, and redistribution of elements, altering physical and chemical processes and directly affecting biological distribution. This process enables water to shape the environment by imprinting its unique characteristics (ARTUR et al., 2014; WESTALL; BRACK, 2018; JARDIM et al., 2020; FONTANA et al., 2022; SILVA et al., 2024).

As water enters terrestrial systems through precipitation, soils and rocks act as dynamic reservoirs of water volumes. These reservoirs influence the forms and velocities of water movement. The result, in the form of runoff, infiltration, percolation, and storage, affects water availability in different environments (MENEZES et al., 2009; HOFFMANN et al., 2022).

Understanding water infiltration rates and their relationship to soil properties permits determining drainage and surface runoff rates (NERY et al., 2017; FLACH et al., 2020; VIDALETTI et al., 2021), facilitating the comprehension of water movement across landscapes and related processes.

In this context, the study of natural environments reveals the characteristics of soil properties and water dynamics in an original setting (JUHÁSZ, 2006). These studies form the basis for understanding the functioning of natural systems, providing a reference for implementing corrective measures in anthropized areas. However, obtaining hydrogeomorphological data in field environments is complex with various factors affecting the time, characteristics, and costs of these experiments. An alternative to expedite data acquisition involves using devices known as infiltrometers, which are categorized as ponded infiltrometers and rainfall simulators.

Ponded infiltrometers involve the use of graduated volume cylinders inserted into the soil. The operation involves flooding a designated area, following the insertion of the cylinders, with water, allowing for the

ISSN eletrônico 2177-2738
RA'EGA, Curitiba, PR, V.61, n.1, p. 29 – 47, 12/2024
http://dx.doi.org/10.5380/raega.v61i1.96603

measurement of water infiltration through soil pores over a specified time, thus revealing the maximum infiltration capacity (NASCIMENTO et al., 2020).

Rainfall simulators, on the other hand, aim to replicate natural precipitation artificially by applying water in droplet form onto the surface, simulating natural rainfall (KOCK et al., 2023). This method also replicates raindrop-dependent processes, closely mimicking natural conditions and their effects (DUNKERLY, 2008; KOCH et al., 2024), providing a more comprehensive study.

However, merely producing droplets does not qualify a device as a rainfall simulator, since real precipitation events have intrinsic characteristics. To ensure reliable use, minimum parameters for calibrating rainfall simulators as hydrogeomorphological data acquisition tools have been established (LORA et al., 2016; CONFESSOR et al., 2022). These parameters ensure that simulated rainfall reflects attributes similar to natural precipitation (LAZARUS et al., 2023).

The criteria for measuring infiltration rates include: continuous water application over the test area; a wet area of more than 0.50 m^2; uniform precipitation distribution with a Christiansen uniformity coefficient (CUC) above 80%; droplets with an average diameter similar to natural ones; droplets impacting the surface at a terminal velocity similar to natural droplets of the same diameterwith a minimum kinetic energy ratio of 75%; and intensity levels representative of the geographic regions under study (ALVES SOBRINHO et al., 2002; CONFESSOR; RODRIGUES, 2018; MACEDO et al., 2021; KUSUMANDARI et al., 2021; CONFESSOR et al., 2024a).

This study aimed to understand the water dynamics in a Regolithic Neosol developed in the Cerrado, within the conservation unit of Serra da Canastra National Park, MG. Primary field data were collected using infiltrometers (rainfall simulator and concentric ring infiltrometer) and the results were compared with other landscape factors such as relief, soils, vegetation, and lithology.

II. Materials and Methods

The study area is located on a slope at coordinates (20°13'59.90"S - 46°36'14.31"W), within the regional context of the Mountain Ranges of the Serra da Canastra National Park (RODRIGUES et al., 2023). To analyze the area's water dynamics, two different types of infiltrometers were used: a Rainfall Simulator to investigate soil behavior under high-intensity precipitation and a concentric ring infiltrometer to assess the soil's total infiltration capacity.

The Rainfall Simulator was constructed based on the model presented by Luck et al. (1986) and was calibrated to accurately replicate the characteristics of simulated rainfall within necessary scientific parameters.

ISSN eletrônico 2177-2738
RA'EGA, Curitiba, PR, V.61, n.1, p. 29 – 47, 12/2024
http://dx.doi.org/10.5380/raega.v61i1.96603

To simulate high-intensity precipitation similar to that in the study area, the equipment was calibrated based on data from the Vargem Bonita Climatological Station (2046013) (Confessor, 2023). Analysis of 46 years of precipitation data and a regression curve of erosive rainfall volumes (>10 mm) established an intensity of 53.9 mm/h as a reference value for the equipment.

Using a 27 wsq spray nozzle (Spraying Systems) positioned at a height of 2.65 meters and an operating pressure of 10 psi, the rainfall simulator replicated precipitation at an intensity of 57.4 mm/h, with a droplet diameter of 1.51 mm (D50), achieving a kinetic energy ratio of 101% between produced and natural droplets of the same diameter, and a uniformity coefficient (CUC) of 94.9%. Details on assembly and calibration procedures can be found in Confessor (2023).

To validate the collected data, the methodology was based on studies by Mhaske et al. (2019), Macedo et al. (2021), and Salem e Meselhy (2021). These studies considered three repetitions sufficient for reliable evaluation. Thus, three replicates of precipitation were applied at different locations on the slope. A 70x100 cm plot (SOBRINHO et al., 2008) was used to define the data collection area for the rainfall simulator, where surface runoff volumes were collected every 5 minutes for up to 60 minutes, totaling 12 samples per experiment.

To determine the soil's maximum infiltration capacity, a semi-automatic concentric ring infiltrometer with low-variable head was used (Figure 1) (CONFESSOR et al., 2024). The device maintained a 5 cm water column over the soil surface for 3 hours (CONFESSOR, 2023). Infiltration values were recorded in 10-minute intervals, totaling 18 samples. Three experiments were conducted at the study area (ROCHETA et al., 2015), with sampling points selected randomly (Figure 1).

ISSN eletrônico 2177-2738
RA'EGA, Curitiba, PR, V.61, n.1, p. 29 – 47, 12/2024
http://dx.doi.org/10.5380/raega.v61i1.96603

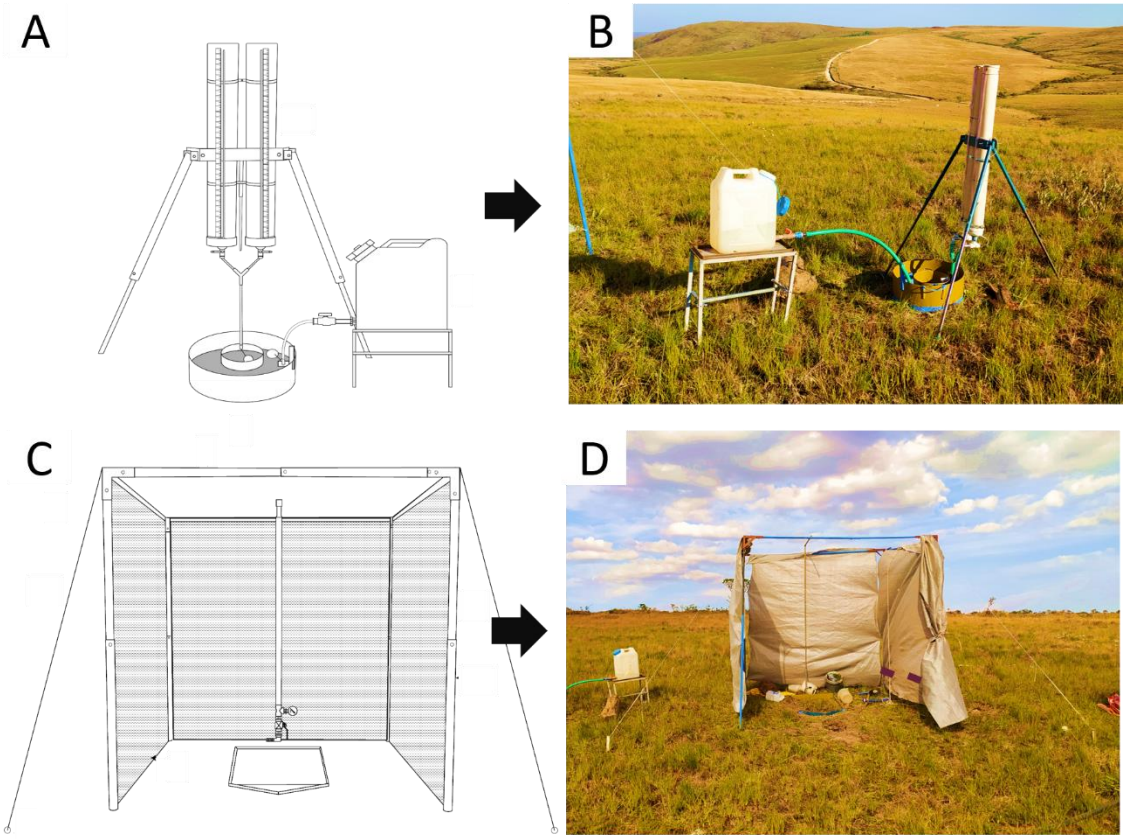

Figure 1 - Equipment used in the research. Semi-automatic concentric ring infiltrometer with low-variable head (A and B); Rainfall simulator and wind protection (C and D). Source: Authors.

Vegetation cover assessment was conducted using ENVI 4.2 softwares, employing supervised image classification. Images of the plots' surface were captured at a height of 1 meter before the rain simulations. The images were then processed to highlight the relationship between exposed soil and vegetative cover (PINESE et al., 2008).

The soil was classified by opening a profile, using the Brazilian soil classification system as a reference (SANTOS, 2018). To determine its physical properties (Total density, Particle density, Granulometry, and total porosity), samples were collected randomly from four points across the experimental area and processed according to manuals (TEIXEIRA et al., 2017).

Undisturbed samples were taken from the surface (0-5 cm) to determine total soil density, particle density, and total porosity. Disturbed samples were collected from the subsurface at uniform intervals of 10 cm down to 50 cm (5 samples per point) to assess granulometric characteristics.

To investigate soil water loss through evaporation, three undisturbed samples were collected at a depth of 0-5 cm using 100 cm^3 volumetric rings. The samples were submerged in water for 2 hours, drained, and

ISSN eletrônico 2177-2738
RA'EGA, Curitiba, PR, V.61, n.1, p. 29 – 47, 12/2024
http://dx.doi.org/10.5380/raega.v61i1.96603

weighed after 1 hour. Subsequently, they were weighed every 24 hours over six days (CONFESSOR, 2023). Water loss was monitored by the weight change from the initial to subsequent samples.

III. Results and Discussion

The study slope is 1 kilometer long with an elevation difference of 80 meters from the top to the valley bottom. It features varying levels of slope, soil types, and vegetation cover along its length. The area under analysis occupies a narrow part of its upper third (Figure 2- B), located in the transition between a gentle slope at the top and steeper on the rest of the slope, with an average gradient of 7.8%.

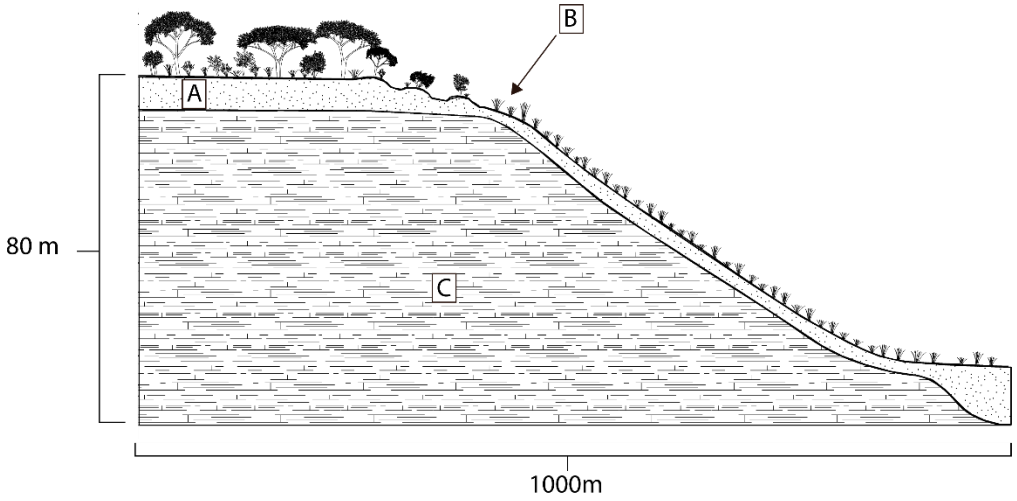

Figure 2 - Diagram of the study slope. Distribution of soil depth (A); Study point (B); Rock (C). Source: Authors.

The vegetation covering the area consists of a set of low-growing plants, primarily grasses and herbaceous species, with average heights predominantly below 30 centimeters. This forms a "clean field" phytophysiognomy characterized by a heterogeneous assemblage of plants (Figure 3). The diverse plant composition includes a mix of low-stature species found in the surrounding areas, displaying a varied array of plants and serves as a transitional area represented by a mix of narrow-leaved and broad-leaved species.

ISSN eletrônico 2177-2738
RA'EGA, Curitiba, PR, V.61, n.1, p. 29 – 47, 12/2024
http://dx.doi.org/10.5380/raega.v61i1.96603

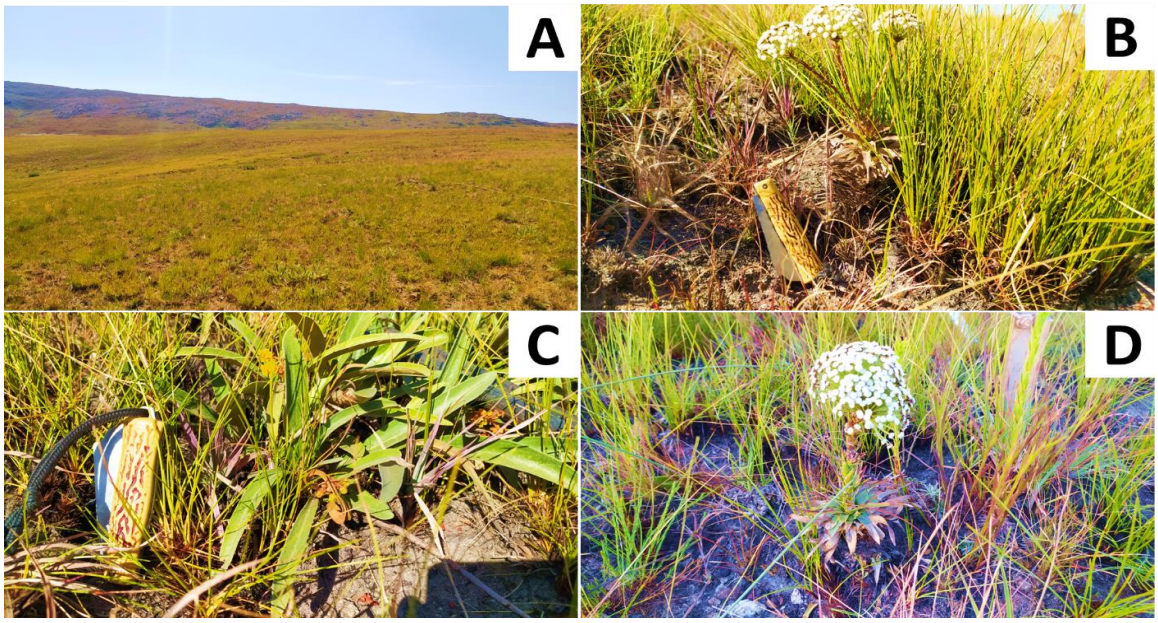

Figure 3 - Characteristics of the vegetation in the study area. Low-growing clean field vegetation (A); Heterogeneous composition of low-growing species (B; C; D). Source: Authors.

The different forms, structural arrangements, and growth habits of the plants produced a vegetation cover with various stratus including different leaf and root structures. Despite the study being conducted during the region's dry season, only a small portion of the vegetation displayed dry structures, with most of the vegetative assemblage having green leaves, and in some cases, flowering species. Despite the variety, low soil cover values were observed, with an average of 40.61% (Figure 4).

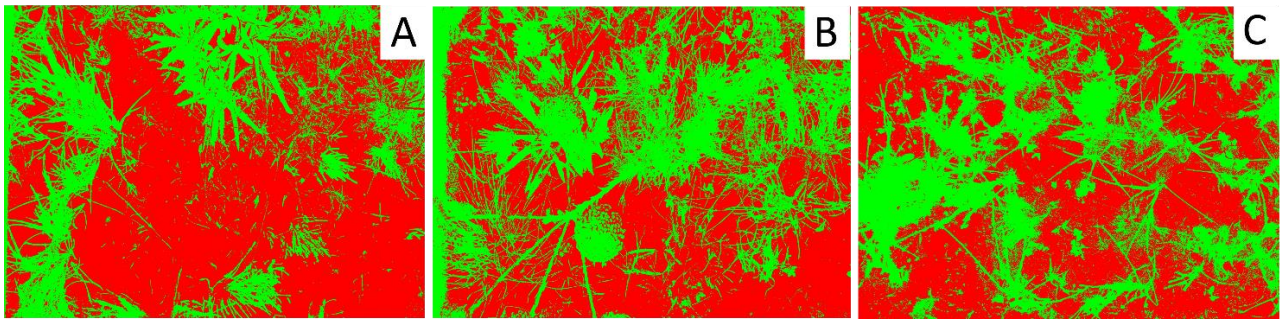

Figure 4 - Relationship between vegetation cover and exposed soil in experimental areas. Exposed soil (red)/Vegetation cover (green). Figure A- 71.18% exposed soil; Figure B- 70.59% exposed soil; Figure C- 65.81% exposed soil. Source: Authors.

The low stature, presence of dry structures, sparse growth between plants, and the predominance of narrow-leaved individuals contributed to the low cover values observed. Additionally, the area did not present a layer of litter on the surface, a result of frequent burning in the region.

The local soil, classified as typical Dystrophic Regolithic Neosol, is shallow with an average depth of 20 centimeters, and is structured over quarzitic rock. It is characterized by a surface horizon approximately 5

ISSN eletrônico 2177-2738
RA'EGA, Curitiba, PR, V.61, n.1, p. 29 – 47, 12/2024
http://dx.doi.org/10.5380/raega.v61i1.96603

centimeters thick, composed of sandy material overlaying a layer of rounded gravel with petrified ferruginous concretions (petroplinthite), abundant with an average diameter of 5 mm (Figure 5).

In areas where erosive processes have removed materials, the gravel has been exhumed and is scattered on the surface among the vegetation. Low-frequency occurrences of concretionary material slabs on the surface were also observed with concretions up to 10 centimeters in diameter among smaller gravel.

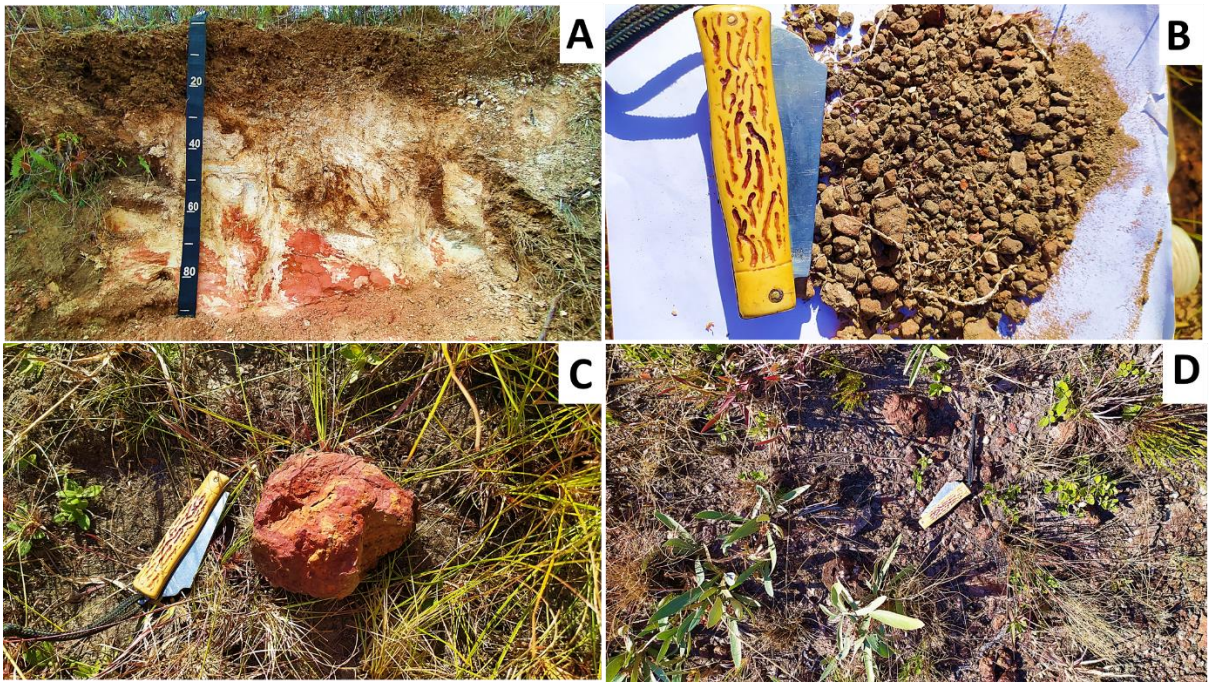

Figure 5 - Characteristics of the local soil. Soil profile with poorly graded granulometry (A); Abundant petroplinthite gravel at depths below 10 cm (B); Ferruginous concretion 10 cm in diameter (C); Exhumed gravel on the surface (D). Source: Authors.

The granulometry revealed poorly graded soils, showing that the surface layer (0-10 cm) contains predominantly fine-grained material (62.1% less than gravel) compared to the underlying layer (10-20 cm), which contains 66.2% gravel (Figure 6). The coarse matrix combined with low clay content in both layers (12.3% and 6.7%) produced a soil with low aggregation, resulting in a poorly structured material with lateritic gravel mixed with finer materials, mainly sand.

ISSN eletrônico 2177-2738
RA'EGA, Curitiba, PR, V.61, n.1, p. 29 – 47, 12/2024
http://dx.doi.org/10.5380/raega.v61i1.96603

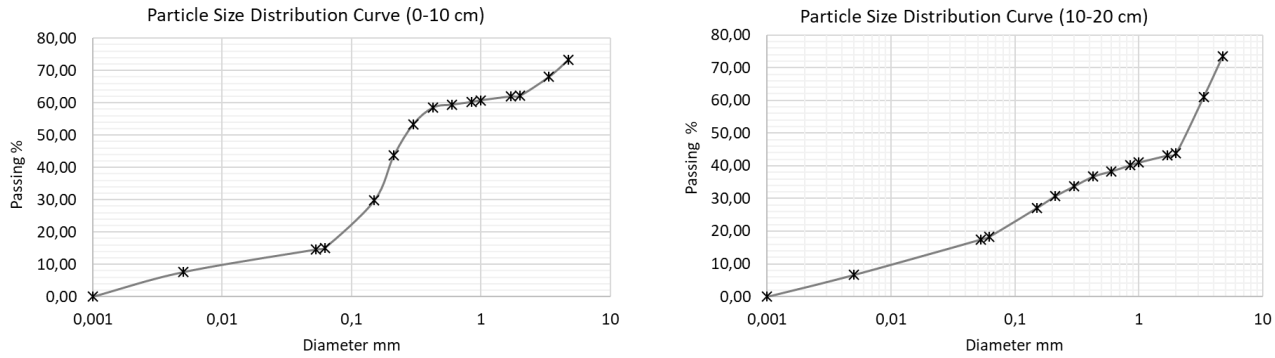

Figure 6 - Grain Size Distribution Curves. Cu-Uniformity Coefficient; Cc-Curvature Coefficient. Source: Authors.

The soil exhibited weak aggregate structure, with total density (Dt) values indicating that the soil in the area is not compacted, showing values below the critical limit of 1.81 (Dt) reported by Reichert et al. (2007), and resulting in a porosity above the ideal limit of 0.50 as stipulated by Kiehl (1979) (Table 1).

The low Dt values and high porosity values are linked to the variable grain size composition, mainly due to the chaotic arrangement of particles of different sizes throughout the profile, particularly the large presence of rounded lateritic gravel.

Table 1- Physical Soil Analysis; Dp- Particle Density; Dt – Total Density; Pt- Total Porosity.

Dp (g/cm^3)	Dt (g/cm^3)	Pt (%)
2,27	1,09	0,52

Source: Authors.

The data obtained from the ring infiltrometer revealed an initial peak infiltration rate of 694.72 mm/h for the local soil (Figure 7), stabilizing after 60 minutes of experiments with a basic infiltration rate (VIB) of 317.58 mm/h. According to Fagundes et al. (2006), rates above 30 mm/h are considered very high.

Comparing the VIB values of the study area with volumes presented in other areas on the same slope (top of the slope - 626.56 mm/h; mid-slope - 22.5 mm/h; and valley bottom - 50.74 mm/h - CONFESSOR et al., 2024c; CONFESSOR et al., 2024d; CONFESSOR et al., 2024e), it is noted that the physiographic attributes of the study area contributed to the formation of favorable conditions for water infiltration into the soil, revealing rates much higher than those observed in other locations on the slope.

The variation in infiltration rate values between the beginning and the end of the experiments was 57.43%, indicating that this environment has a high capacity for water infiltration and percolation into the soil profile, even when saturated for long periods, with a correlation of $R^2 = 0.88$ for the infiltration curve values.

ISSN eletrônico 2177-2738
RA'EGA, Curitiba, PR, V.61, n.1, p. 29 – 47, 12/2024
http://dx.doi.org/10.5380/raega.v61i1.96603

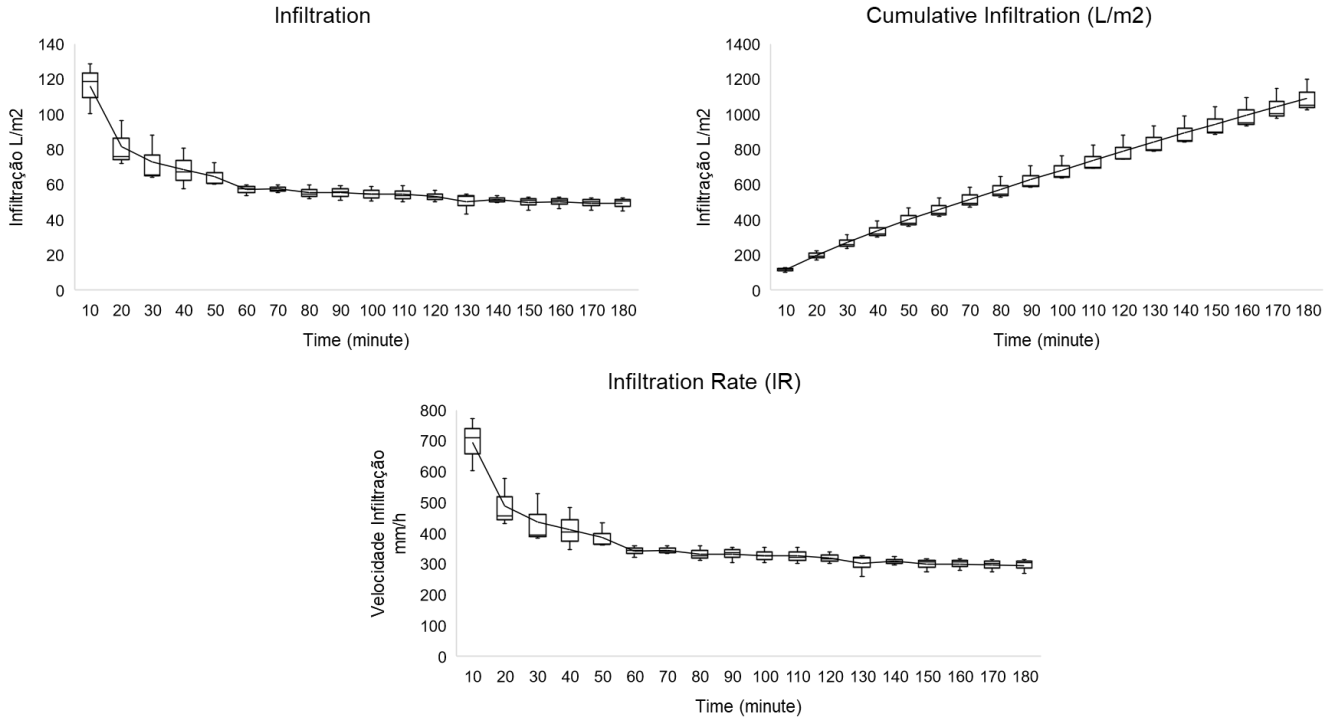

Figure 7 - Infiltration from ring infiltrometer. Source: Authors.

The experiments using the rainfall simulator revealed that surface runoff began at 11:50 minutes after the onset of precipitation, generating an initial abstraction of 11.32 mm, representing 19.72% of the total precipitation during the experiments. Despite the onset of runoff, the flow ceased at 50 minutes into the tests, and the precipitation returned to complete infiltration.

The infiltrating water in the soil profile may have unclogged potential pores, inducing the formation of preferential channels for flow percolation, reducing surface runoff rates and increasing infiltration, resulting in low correlation values for the runoff curve, $R^2 = 0.08$ (Figure 8).

Overall, only 0.69% of the total precipitation (0.39 liters) was runoff, indicating that this environment has a high-water retention capacity, even under high-intensity precipitation. This finding is confirmed by comparing the runoff volumes in lower areas of the slope, which showed volumes of 17.4 liters in the mid-slope and 13.62 liters in the valley bottom (CONFESSOR et al., 2024d, 2024e), similar to the area at the top, which showed no runoff (CONFESSOR et al., 2024c).

ISSN eletrônico 2177-2738
RA'EGA, Curitiba, PR, V.61, n.1, p. 29 – 47, 12/2024
http://dx.doi.org/10.5380/raega.v61i1.96603

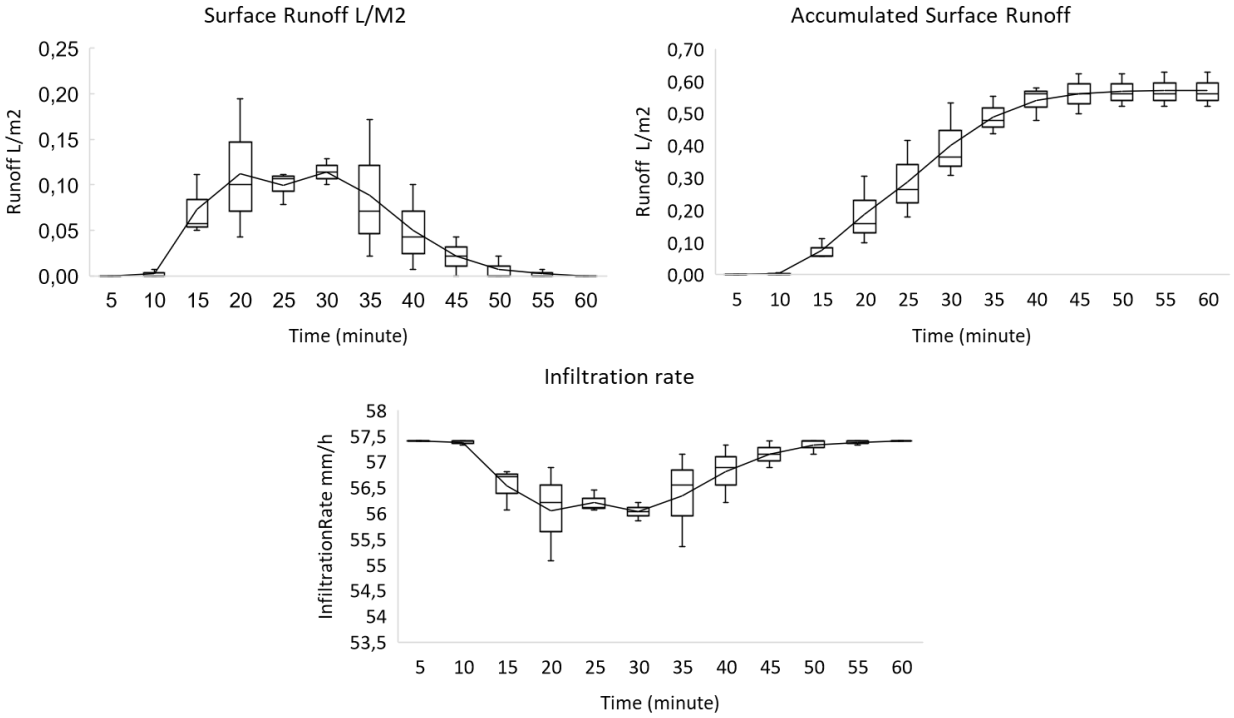

Figure 8 - Runoff and infiltration curves produced by the rainfall simulator. Source: Authors.

After saturation, the soil exhibited a storage capacity of 0.72 ml/cm³, with water losses due to evaporation decreasing steadily over time. A total volume of 0.37 ml/cm³ was evaporated over six days, corresponding to 56.16% of all water retained in the soil (Figure 9).

The highest volumes of evaporation were observed in the first 96 hours, with 88.81% of the total during this period. Thus, the soil showed a water retention capacity (CRA) of 0.37 ml/cm³ at the end of six days, representing 43.83% of its totais storage capacity. This indicated a rapid recovery of its empty spaces, enabling it to incorporate new inputs from subsequent precipitation.

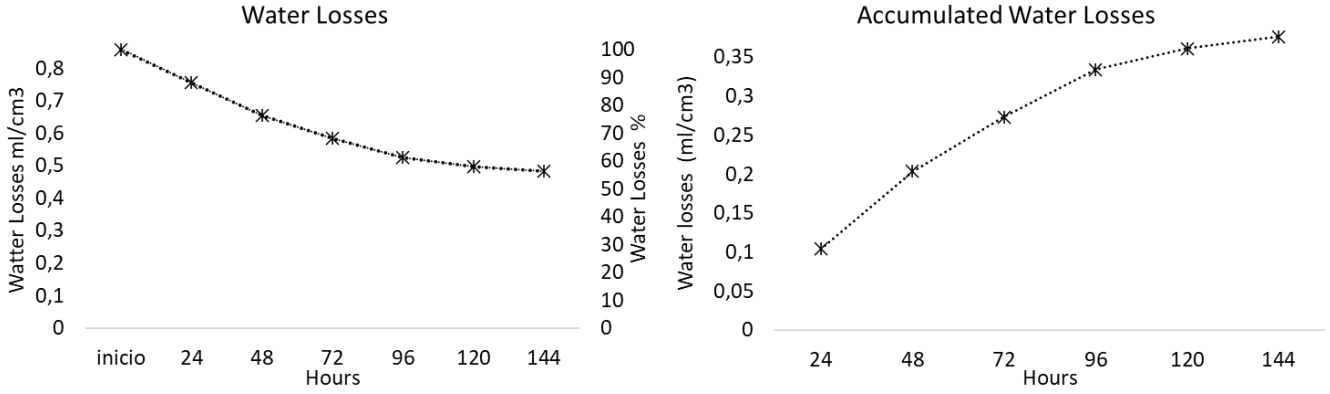

Figure 9 - Water Loss by Evaporation. Source: Authors.

ISSN eletrônico 2177-2738
RA'EGA, Curitiba, PR, V.61, n.1, p. 29 – 47, 12/2024
http://dx.doi.org/10.5380/raega.v61i1.96603

Overall, the area exhibited a high infiltration capacity, where the grain size composition of the soil matrix in its different layers contributed to the formation of environments with good porosity, providing preferential channels for the downward movement of water in the soil profile.

The sandy surface layer allowed for the infiltration of volumes, and the lateritic gravel layer facilitated percolation within the profile, creating environments for the movement of water at depths, quickly directing it, without resistance, to the downward infiltration flow.

Despite the shallow soil, the contact between the gravel layer and the underlying quartzitic rock acted as a drainage layer, redirecting the water flow direction from vertically downward to horizontal (Figure 10), contributing to the high VIB values observed.

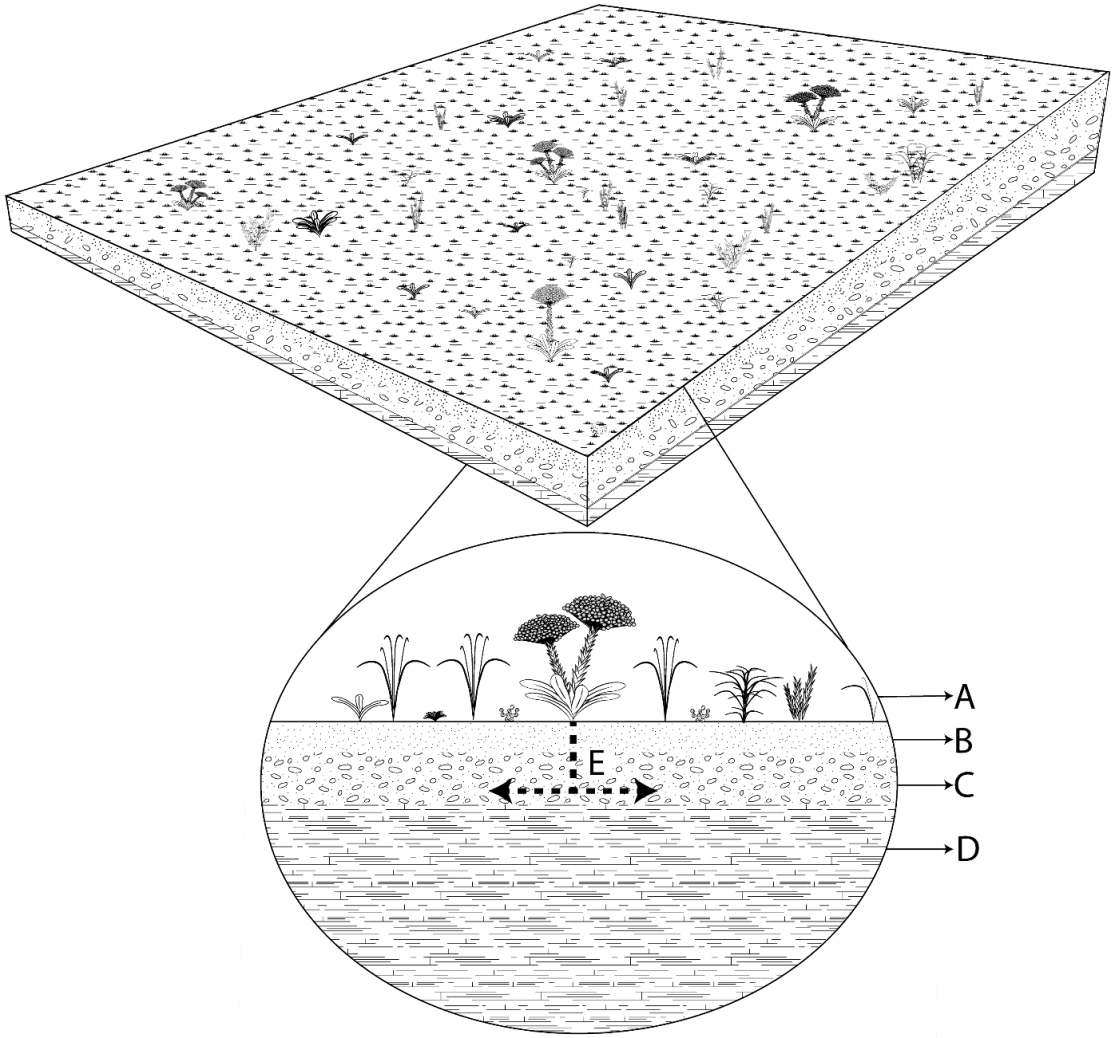

Figure 10 - Diagram of the study area. Heterogeneous low-growing vegetation cover (A); Sandy soil layer (B); Lateritic gravel layer (C); Quartzitic rock (D); Water flow direction in the soil profile. Source: Authors.

ISSN eletrônico 2177-2738
RA'EGA, Curitiba, PR, V.61, n.1, p. 29 – 47, 12/2024
http://dx.doi.org/10.5380/raega.v61i1.96603

Throughout the area, where erosive processes have exhumed the quartzitic rock, subsurface water flows were observed draining from the gravel layer in contact with the rock, indicating the ease of water movement in this soil horizon (Figure 11).

The significant presence of rounded lateritic gravel suggests that the area serves as a site for pedogenetic processes of material formation and/or deposition. The high soil permeability creates environments for redox reactions, where the porous spaces incorporate air into the soil, oxygenating the subsurface flows and oxidizing the iron dissolved in the water solution.

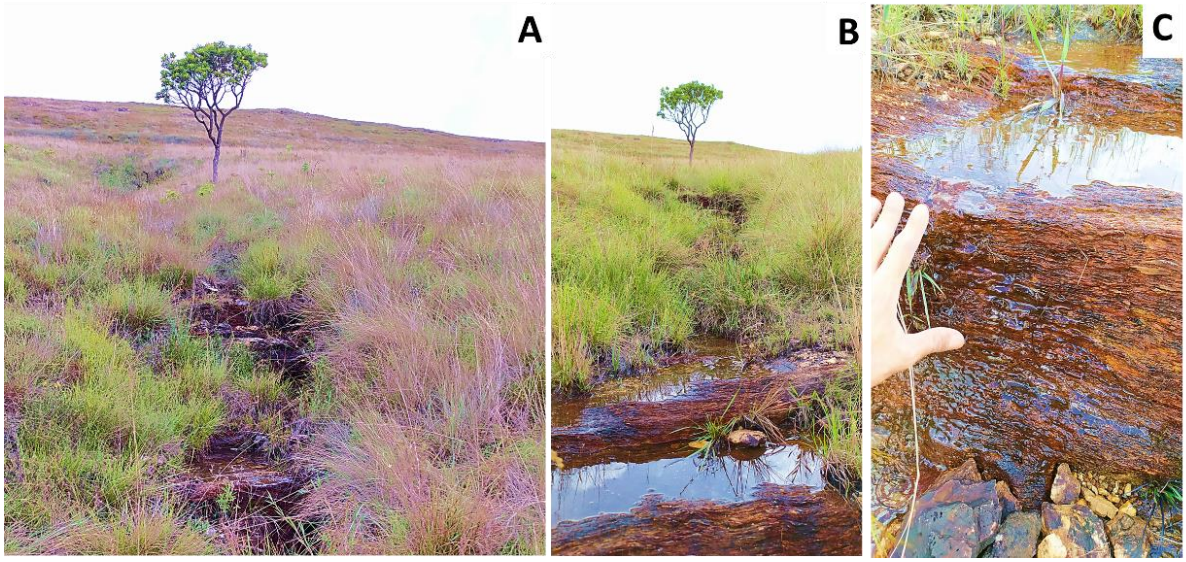

Figure 11 - Water exfiltration movement. Erosive channel (A); Water exfiltration (B and C). Source: Authors.

The oxidation of iron precipitates this element into the sandy matrix, binding the particles together to form lateritic gravel. This gravel is predominantly found at depths near the contact with the rock, where fluctuations in the water table occur more frequently, contributing to the formation of the gravel layer reported in the area.

The presence of lateritic crust on the surface indicates that the environment has undergone erosion processes, with the valley expanding through the removal of materials and causing the retreat of the slope. However, the layers of lateritic crust act as barriers against the upward erosion in the system, as they are resistant to chemical and physical weathering (OLIVEIRA, 2003; MAKLUR; NARKHEDE, 2018).

In this sense, the erosive retreat of the slope is halted at this location, creating a noticeable difference in the slope gradient between the areas above and below, with steeper relief downstream and gentler relief

ISSN eletrônico 2177-2738
RA'EGA, Curitiba, PR, V.61, n.1, p. 29 – 47, 12/2024
http://dx.doi.org/10.5380/raega.v61i1.96603

upstream. The prevention of erosion at this specific point protects the environments above, preserving the processes that occur within them.

IV. CONCLUSIONS

In summary, the study area describes a transitional location on the slope, situated between the flat top and the steeper areas further down. Its position on the slope directly influenced the environmental variables found, affecting the vegetation composition, water movement, soil formation and structure processes.

Classified as a typical Dystric Lithic Regosol, the soil developed over quartzite bedrock is shallow and exhibits varied grain sizes, with a predominance of rounded lateritic gravel and sand, resulting in low aggregation and high porosity. These attributes provide a high infiltration capacity, as evidenced by low surface runoff values (0.39 liters) even under simulated high-intensity rainfall (57.4 mm/h), with the ring infiltrometer revealing high infiltration rates (317.58 mm/h).

Due to its high permeability, shallow depth, and presence over less porous quartzite rock, the infiltrated water moves vertically through the soil until reaching the lithic contact, then flows laterally over the rock towards lower parts of the slope. After saturation, the soil exhibited a high capacity to restore its porosity, allowing for the incorporation of new inputs. These characteristics indicate that this environment acts as a transitional area for water flows, channeling them subsurface between the upper slope and the valley bottom.

The presence of exhumed lateritic gravel and ferruginous slabs on the surface indicates active erosion processes in specific areas. However, the layers of lateritic crust play a crucial role in protecting the upper slope soils from upslope erosion, reducing material loss through their chemical and mechanical resistance, thereby contributing to the preservation of the environments and associated processes further upslope.

These factors influenced the biological occupation, directly affecting the vegetation composition, which exhibited a clean field phytophysiognomy, with low-stature plants mainly composed of grasses and herbaceous species.

Finally, it can be concluded that the study area presents a complex interaction between geological, vegetative, and pedological elements, resulting in an environment with high infiltration capacity, resistance to erosion, and an efficient response to precipitation events.

ISSN eletrônico 2177-2738
RA'EGA, Curitiba, PR, V.61, n.1, p. 29 – 47, 12/2024
http://dx.doi.org/10.5380/raega.v61i1.96603

Acknowledgements

We would like to express our gratitude to CAPES for the doutoral scholarship granted to the first author, as well as for the partial funding of this research provided by CNPQ, through PQ Scholarship 302924/2019-1 andUniversal Grant 403412/2023-4, and the CAPES/UFU/PRINT Project 88887.311520/2018-00.

V. REFERENCES

ALVES SOBRINHO, T.; GÓMEZ-MACPHERSON, H.; GÓMEZ, J. A. A portable integrated rainfall and overland flow simulator. Soil Use and Management, 24(2), 163–170, 2008. DOI:10.1111/j.1475-2743.2008.00150.x.

ARTUR, G.; OLIVEIRA, P.; COSTA, G.; ROMERO, E.; SILVA, C.; FERREIRA, O. Variabilidade espacial dos atributos químicos do solo, associada ao microrrelevo. Revista Brasileira de Engenharia Agrícola e Ambiental, 18(2), 141–149, 2014. DOI:10.1590/s1415-43662014000200003.

CONFESSOR, J. G. Dinâmica hidrogeomorfológica de vertentes do Chapadão do Diamante - Serra da Canastra – MG. Tese (Doutorado em Geografia), 231 f. Universidade Federal de Uberlândia, Uberlândia, 2023. DOI: http://doi.org/10.14393/ufu.te.2023.70.

CONFESSOR, J. G.; CARVALHO, F.; RODRIGUES, S. C. Desenvolvimento, calibração e validação de um simulador de chuvas aplicado a estudos hidrogeomorfológicos. GEOGRAFIA (Londrina), 31(2), 233, 2022. DOI:10.5433/2447-1747.2022v31n2p233.

CONFESSOR, J. G.; RODRIGUES, S. C. Método para calibração, validação e utilização de simuladores de chuvas aplicados a estudos hidrogeomorfológicos em parcelas de erosão. Revista Brasileira De Geomorfologia, 19(1), 2018. DOI: https://doi.org/10.20502/rbg.v19i1.1294.

CONFESSOR, J. G.; SILVA, L. L.; RODRIGUES, S. C. Dinâmica hídrica do solo de fitofisionomia de campo limpo do Parque Nacional da Serra da Canastra-MG. Caderno de Geografia, v. 34 n. 76, 2024d. DOI: https://doi.org/10.5752/P.2318-2962.2024v34n76p286.

CONFESSOR, J. G.; SILVA, L. L.; RODRIGUES, S. C. Dinâmica hídrica do solo de fitofisionomia de Cerrado Ralo do Chapadão do Diamante - Serra da Canastra (MG). Mercator, v23, 2024c. DOI https://doi.org/10.4215/rm2024.e23006.

CONFESSOR, J. G.; SILVA; LIMA, N. A.; SANTOS, A. B. P. Dinâmica Hídrica do Solo de Zona Ripária do Chapadão do Diamante – Serra da Canastra, Minas Gerais. Sociedade e Natureza, 2024e. DOI: 10.14393/SN-v36-2024-72336.

CONFESSOR, J. G.; SILVA, L. L.; RODRIGUES, S. C. R. Infiltrômetro de anéis duplos semiautomático de carga pouco variável. Revista Brasileira de Geografia, v. 69, n. 1, p. 69-84, 2024b. DOI: https://doi.org/10.21579/issn.2526-0375_2024_n1_69-84.

CONFESSOR, J. G.; SILVA, L. L.; RODRIGUES, S. C. Simuladores de Chuvas: convergência entre parâmetros científicos e de uso na replicação da precipitação natural. Revista da Casa da Geografia de Sobral (RCGS), [S. l.], v. 26, n. 3, p. 1–26, 2024a. DOI: 10.35701/rcgs.v26.1001.

ISSN eletrônico 2177-2738
RA'EGA, Curitiba, PR, V.61, n.1, p. 29 – 47, 12/2024
http://dx.doi.org/10.5380/raega.v61i1.96603

FAGUNDES, E.; KOETZ, M.; RUDEL, N.; SANTOS, T.; PORTO, R. Determinação da infiltração e velocidade de infiltração de água pelo método de infiltrômetro de anel em solo de cerrado no município de Rondonópolis-MT. Enciclopédia biosfera, 8(14), 2012.

FLACH, C. W.; ALVES, E. A. C.; MEURER, M. Taxa de infiltração da água e resistência mecânica à penetração em solos submetidos a diferentes usos na região da serra de sudeste/RS. Revista Caminhos de Geografia, 21(73), 223-242, 2020. DOI: https://doi.org/10.14393/RCG217348139.

FONTANA, A. C.; SILVEIRA, H.; MARCATTO, F. S.; NÓBREGA, M. T. Caracterização e Comportamento Físico-Hídricos Do Sistema Pedológico Da Topossequência De Solos Dourados, Cambira, Pr, Brasil. RAEGA - O Espaço Geográfico Em Análise, 53, 182, 2022. DOI: https://doi.org/10.5380/raega.v53i0.79511.

HOFFMANN, G. P.; FRANKE, A. E.; NANNI, A. S. Efeitos da modificação do uso e cobertura da terra no comportamento da recarga e descarga em uma porção do Sistema Aquífero Integrado Guarani/Serra Geral. RA'EGA, V.54, p. 81-101, 2022. DOI: http://dx.doi.org/10.5380/raega.v54i0.75297.

JARDIM, A. M. D. R. F.; SILVA, T. G. F.; SOUZA, L. S. B.; ALVES, H. K. M. N.; ARAÚJO, J. F. N.; SILVA, G. I. N.; DA SILVA, J. O. N. Dinâmica da água no solo com cultivo de palma forrageira sob quatro sistemas de plantio. Agrometeoros, v. 27, n. 2, 2020. DOI: http://dx.doi.org/10.31062/agrom.v27i2.26446.

JUHÁSZ, C. E. P.; CURSI, P. R.; COOPER, M.; OLIVEIRA, T. C.; RODRIGUES, R. R. Dinâmica físico-hídrica de uma topossequência de solos sob Savana Florestada (Cerradão) em Assis, SP. Revista Brasileira de Ciência Do Solo, 30(3), 401–412, 2006. DOI: https://doi.org/10.1590/s0100-06832006000300002.

KIEHL, E. J. Manual de edafologia: relações solo-planta. São Paulo: Ceres, 1979.

KOCH, T.; CHIFFLARD, P.; ARTSMA, P.; PANTEN, K. A review of the characteristics of rainfall simulators in soil erosion research studies. MethodsX, 12(102506), 102506, 2024. DOI:10.1016/j.mex.2023.102506.

KOCH, T.; CHIFFLARD, P.; AARTSMA, P.; PANTEN, K. A review of the characteristics of rainfall simulators in soil erosion research studies. MethodsX, v. 12, n. 102506, 2023. DOI: https://doi.org/10.1016/j.mex.2023.102506.

KUSUMANDARI, A.; SATRIAGASA M. C.; HADI PURWANTO, R.; WIDAYANTI, W. T. Erosion Measurement by Using Rainfall Simulator at Grass Soil and after Harvested Soil in Wanagama. IOP Conference Series: Earth and Environmental Science, 810, 2021. DOI:https://doi.org/10.1088/1755-1315/810/1/012053.

LAZARUS, R. R.; WAN JAAFAR, W. Z.; ALENGARAM, U. J.; HIN, L. S. Overview of the research gaps in the rainfall simulator study. Soil Science Society of America Journal. Soil Science Society of America, 87(6), 1231–1248. 2023. DOI:10.1002/saj2.20590.

LE MAITRE, D. C.; MILTON, S. J.; JARMAIN, C.; COLVIN, C. A.; SAAYMAN, I.; VLOK, J. H. J. Linking ecosystem services and water resources: landscape-scale hydrology of the Little Karoo. Frontiers in Ecology and the Environment, 5(5), 261–270, 2007. DOI: https://doi.org/10.1890/1540-9295(2007)5[261:lesawr]2.0.co;2.

LORA, M.; CAMPORESE, M.; SALANDIN, P. Design and performance of a nozzletype rainfall simulator for landslide triggering experiments. CATENA, v. 140, p. 77–89, 2016. DOI: https://doi.org/10.1016/j.catena.2016.01.018.

LUK, S. HUNG; ABRAHAMS, A. D.; PARSONS, A. J. Methodology: a simple rainfall simulator and trickle system for hydro-geomorphological experiments. Physical Geography, v 7, 1986. DOI: https://doi.org/10.1080/02723646.1986.10642303.

MACEDO, P. M. S.; PINTO, M. F; ALVES SOBRINHO, T.; SCHULTZ, N.; COUTINHO, T.; CARVALHO, D. A modified

ISSN eletrônico 2177-2738
RA'EGA, Curitiba, PR, V.61, n.1, p. 29 – 47, 12/2024
http://dx.doi.org/10.5380/raega.v61i1.96603

portable rainfall simulator for soil erosion assessment under different rainfall patterns. Journal of Hydrology, 596(126052), 126052, 2021. DOI:10.1016/j.jhydrol.2021.126052.

MAKLUR, N.; NARKHEDE, P. Study of laterite stone as building material. International Journal of Engineering Research, 7(special3), 223-226, 2018. DOI: 10.5958/2319-6890.2018.00063.6.

MENEZES, M. D.; JUNQUEIRA JÚNIOR, J. A.; MELLO, C.; SILVA, A.; CURI, N.; MARQUES, J. Dinâmica hidrológica de duas nascentes, associada ao uso do solo, características pedológicas e atributos físico-hídricos na sub-bacia hidrográfica do Ribeirão Lavrinha – Serra da Mantiqueira (MG). Scientia Forestalis, Piracicaba, v. 37, n. 82, p. 175-184, jun. 2009.

MHASKE, S. N.; PATHAK, K.; BASAK, A. A comprehensive design of rainfall simulator for the assessment of soil erosion in the laboratory. CATENA, 172, 408–420, 2019. DOI:10.1016/j.catena.2018.08.039.

NASCIMENTO, L. G. DO; SANTOS, M. E. S.; MELO, S. T.; BUZAR, R. J. C.; RESENDE, M. R.; SOUSA, M. M. A.; SOUSA, R. M. L.; ALVES, K. R. Análise da velocidade de infiltração de água no solo por meio de anéis concêntricos na zona leste da cidade de Teresina - PI / Analysis of the speed of water infiltration in the soil by means of concentric rings in the east of the city of Teresina - PI. Brazilian Journal of Development, 6(3), 15168–15178, 2020. DOI: https://doi.org/10.34117/bjdv6n3-406.

NERY, A. R.; RODRIGUES, L. N.; SOUSA, A. G.; SANTOS, F. F. C.; NERE, D. E. R. Infiltração de água nos solos cultivados com palma forrageira e pastagem no IFCE campus Crato. Acta Kariri Pesq. e Des.,2(1), 56-61, 2017.

OLIVEIRA, L.; caracterização dos latossolos da chapada de Araguari: minerais argilosos, granulometria e evolução. Caminhos de Geografia, 3(7)20-37, Fev/2003.

PINESE, J. F.; CRUZ, L. M.; RODRIGUES, S. C. Monitoramento de erosão laminar em diferentes usos da terra, Uberlândia - MG. Sociedade & Natureza 20, 157-175, 2008.

REICHERT, J. M.; SUZUKI, L. E. A. S.; REINERT, D. J. Compactação do solo em sistemas agropecuários e florestais: identificação, efeitos, limites críticos e mitigação. Sociedade Brasileira de Ciência do Solo, 2007. v. 5p. 49–134.

ROCHETA, V. L. S.; ISIDORO, J. M. G. P.; LIMA, J. L. M. P. Infiltration of Portuguese cobblestone pavements – An exploratory assessment using a double-ring infiltrometer. Urban Water Journal, 14(3), 291–297, 2015. DOI:10.1080/1573062x.2015.1111914.

RODRIGUES, S. C.; AUGUSTIN, C.; NAZAR, T. Mapeamento Geomorfológico do Estado de Minas Gerais: uma proposta com base na morfologia. Revista Brasileira de Geomorfologia, v. 24, n. 1, 2023. DOI: https://doi.org/10.20502/rbg.v24i1.2233.

SALEM, H. M.; MESELHY, A. A. A portable rainfall simulator to evaluate the factors affecting soil erosion in the northwestern coastal zone of Egypt. Nat Hazards 105, 2937–2955, 2021. DOI: https://doi.org/10.1007/s11069-020-04432-8.

SANTOS, H. Sistema brasileiro de classificação de solos. 5 Brasília: EMBRAPA, 356 p. 2018.

SILVA, G. S. F.; ANDRADE JÚNIOR, A. S.; CARDOSO, M. J.; ARAÚJO NETO, R. B. Dinâmica da água no solo e produtividade em consórcio de milho e Brachiaria ruziziensis. Pesquisa Agropecuária Tropical, Goiânia, v. 50, p. e59809, 2020. Disponível em: https://revistas.ufg.br/pat/article/view/59809. Acesso em: 24 jul. 2024.

TEIXEIRA, P. C.; DONAGEMMA, G. K.; FONTANA, A.; TEIXEIRA, W. G. Manual de métodos de análise de solo. Brasília, DF: EMBRAPA, 2017.

ISSN eletrônico 2177-2738
RA'EGA, Curitiba, PR, V.61, n.1, p. 29 – 47, 12/2024
http://dx.doi.org/10.5380/raega.v61i1.96603

VIDALETTI, V. F.; MARINS, A. C.; SECCO, D.; RIZZI, R. L.; CHANG, P. Impact of land cover, slope and precipitation on soil water infiltration. Research, Society and Development, v. 10, n. 17, p. e193101724562, 2021. DOI: https://doi.org/10.33448/rsd-v10i17.24562.

WESTALL, F.; BRACK, A. The Importance of Water for Life. Space Science Reviews, v. 214, p. 1-23, 2018.

O ESPAÇO GEOGRÁFICO EM ANÁLISE
https://revistas.ufpr.br/raega
ISSN eletrônico 2177-2738
RA'EGA, Curitiba, PR, V.61, n.1, p. 29 – 47, 12/2024
http://dx.doi.org/10.5380/raega.v61i1.96603